International Atomic Energy Agency

INDC(CPR)-010/L

INDC INTERNATIONAL NUCLEAR DATA COMMITTEE

GAMMA RAY PRODUCTION CROSS SECTIONS FOR THE INTERACTIONS OF 14.9 MeV NEUTRONS WITH C, Al, V, Fe AND Nb AT 90°

By Zhou Hongyu, Tang Lin, Yan Yiming, Wen Shenlin, Lan Liquiao,
Zhang Shengji, Wang Qi, Sun Shuxu, Han Chongzhan,
Ding Xiaoji and Wang Wanhong
Institute of Low Energy Nuclear Physics
Beijing Normal University, Beijing, China

November 1986

IAEA NUCLEAR DATA SECTION, WAGRAMERSTRASSE 5, A-1400 VIENNA

INDC(CPR)-010/L

GAMMA RAY PRODUCTION CROSS SECTIONS FOR THE INTERACTIONS OF 14.9 MeV NEUTRONS WITH C, Al, V, Fe AND Nb AT 90°

By Zhou Hongyu, Tang Lin, Yan Yiming, Wen Shenlin, Lan Liquiao,
Zhang Shengji, Wang Qi, Sun Shuxu, Han Chongzhan,
Ding Xiaoji and Wang Wanhong
Institute of Low Energy Nuclear Physics
Beijing Normal University, Beijing, China

November 1986

Reproduced by the IAEA in Austria
November 1986

86-06066

GAMMA RAY PRODUCTION CROSS SECTIONS FOR THE INTERACTIONS OF 14.9 MeV NEUTRONS WITH C, Al, V, Fe AND Nb AT 90°

By Zhou Hongyu, Tang Lin, Yan Yiming, Wen Shenlin, Lan Liquiao, Zhang Shengji, Wang Qi, Sun Shuxu, Han Chongzhan, Ding Xiaoji and Wang Wanhong
Institute of Low Energy Nuclear Physics
Beijing Normal University, Beijing, China

Introduction

γ ray production cross sections of fast neutrons are the basic nuclear data for the design of the radiation shield of nuclear plants and the evaluation of γ ray heating of fusion reactors. Discrete γ ray spectra and production cross sections have interest for understanding level structures and mechanisms of nuclear reactions for various nuclides. Because of the above mentioned reasons a pulsed fast neutron time-of-flight(TOF) facility at the Cockcroft-Walton Accelerator is constructed. Discrete γ ray spectra and production cross sections for 14.9MeV neutrons with C, Al, V, Fe, Nb at 90° have been measured.

Experimental Method

The experimental arrangement is presented in Fig.1. 14.9MeV neutrons were produced by the $T(d,n)^4He$ reactions at the Cockcroft Walton Accelerator. 300KeV deuteron beams were first swept by means of a high voltage chopper with repetition ratio of 3.16MHZ both in the horizontal and vertical directions. the chopped heam burst with 15 nsec was obtained and was then passed through a spiral loaded wave guide buncher. The time resolution of the whole pulsing system was about 1 nsec. The averaged pulsed deuteron ion beam current at the target was 3-4μA. Neutron intensity was about 5×10^8 neutron/sec. A capacitive pick-off mounted at the deuteron beam pipeline in 40cm distance from the target was used for generating start time signals. Absolute neutron flux was determined by associated particle counting with a Si(Au) detector at 90° to the deuteron beam axis in 100cm distance from the target with 3.2×10^{-6} steradian. A cylindrical liguid scintillator ST-451 and a NE 111 plastic scintillator were used for monitoring neutron flux.

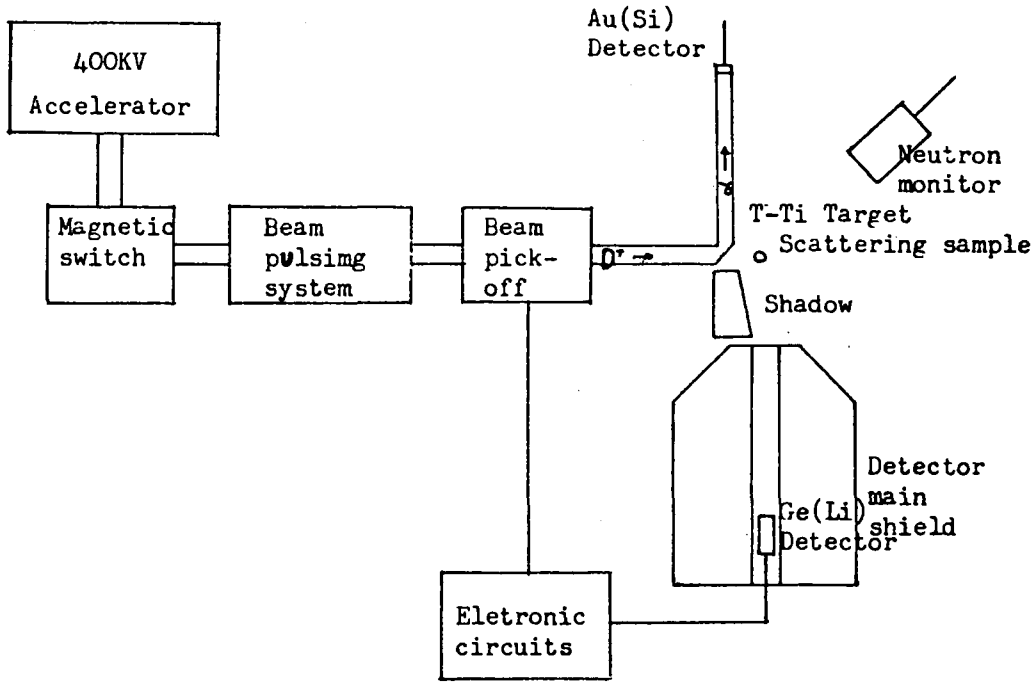

Fig.1 General View of the Experimental Set-up.

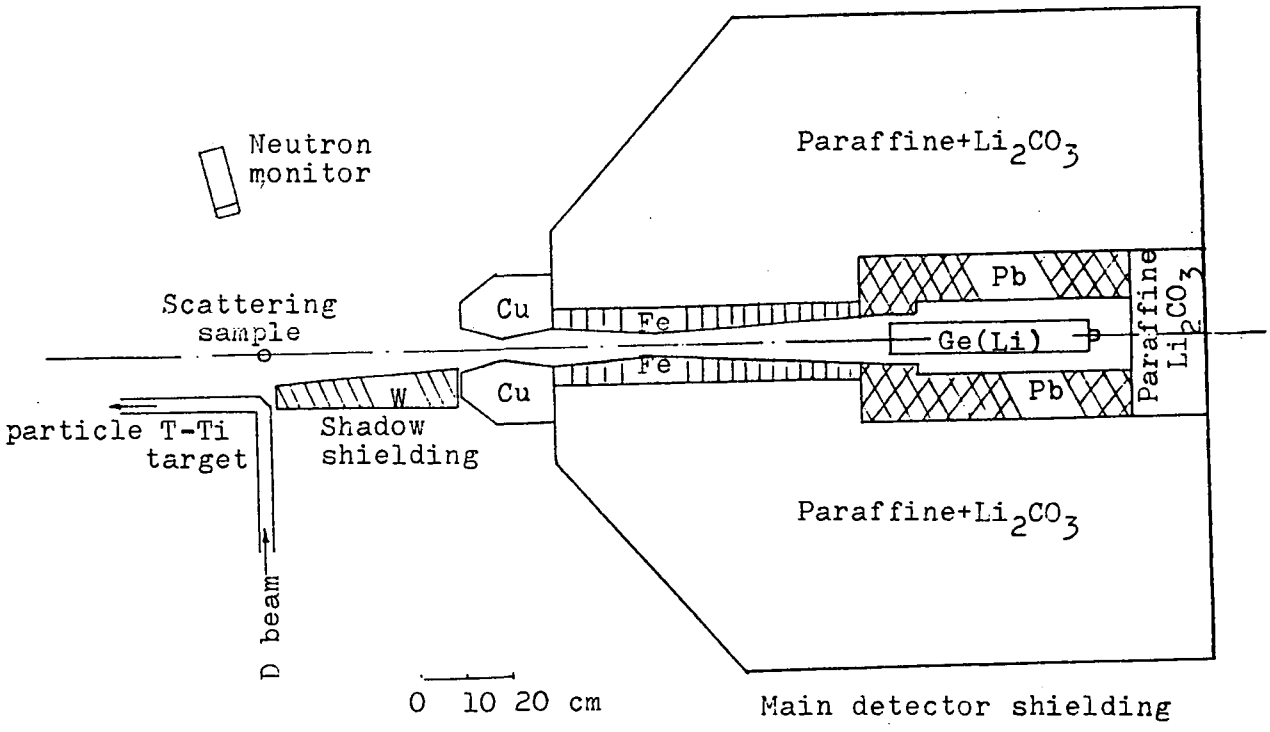

Fig.2 The shielding arrangment for fast neutron scattering measurements.

The samples for Al, V, Fe, Nb were the metals of natural abundances in 3cm diameter, and 3cm high, and the sample for C was natural graphite with similar size and shape. The purity of the samples was in more than 99.9%. The samples were placed at 13.4cm from the neutron target and 0° relative to the deuteron beam axis.

The γ rays produced by interactions of neutrons with the samples were detected by 110.7cm^3 Ge(Li) detector at 139.4cm from the sample and at 90° relative to the axis of the neutron beam incident upon the sample (see Fig.2). The energy resolution of the Ge(Li) spectrometer was 1.85 KeV (FWHM) for γ ray of 1.33MeV, the peak-to-compton ratio was about 50:1, and relative efficiency was 23.5% to NaI(Tl) in 3"x3". The absolute efficiency calibration of the Ge(Li) was carried out with a set of standard sources, such as ^{152}Eu, ^{60}Co, ^{88}Y, ^{137}Cs, ^{241}Am, ^{22}Na, ^{54}Mn, and a set of nonstandard sources, such as ^{24}Na, ^{56}Co, ^{226}Ra, ^{133}Ba, ^{15}N, ^{36}Cl, in which ^{15}N and ^{36}Cl were obtained from radiative capture of thermal neutrons produced in the reactor. The full energy peak efficiency curve from 26KeV to 10.8MeV, and single escape peak and double escape peak efficiency curves from 1.77MeV to 10.8MeV were obtained (see Fig.3). The calibration was carried out at the same distance from the sample to the Ge(Li) detector as in (n,xγ) reaction measurement, so we need not to take the extrapolation of the efficiency, which can produce errors due to the uneertainty of effective centre of the Ge(Li) detector for the γ rays with differeut energy. Therewith the errors produced from the scattering from around objects and other surroundiugs were also eliminated. The multinomial progressively regression method was used in the fitting efficiency curves. The Ge(Li) detector was placed in heavy major shielding which consists of Lithium, carbonate, paraffin wax, lead and iron. There was a shade shielding which consists of iron and tungsten between the neutron target and the major shielding. The shielding efficiency to 14MeV neutrons was about 10^5.

Electronic block diagram is shown in Fig.4. The experimental conditions were carefully selected and some measures were adopted to ensure the

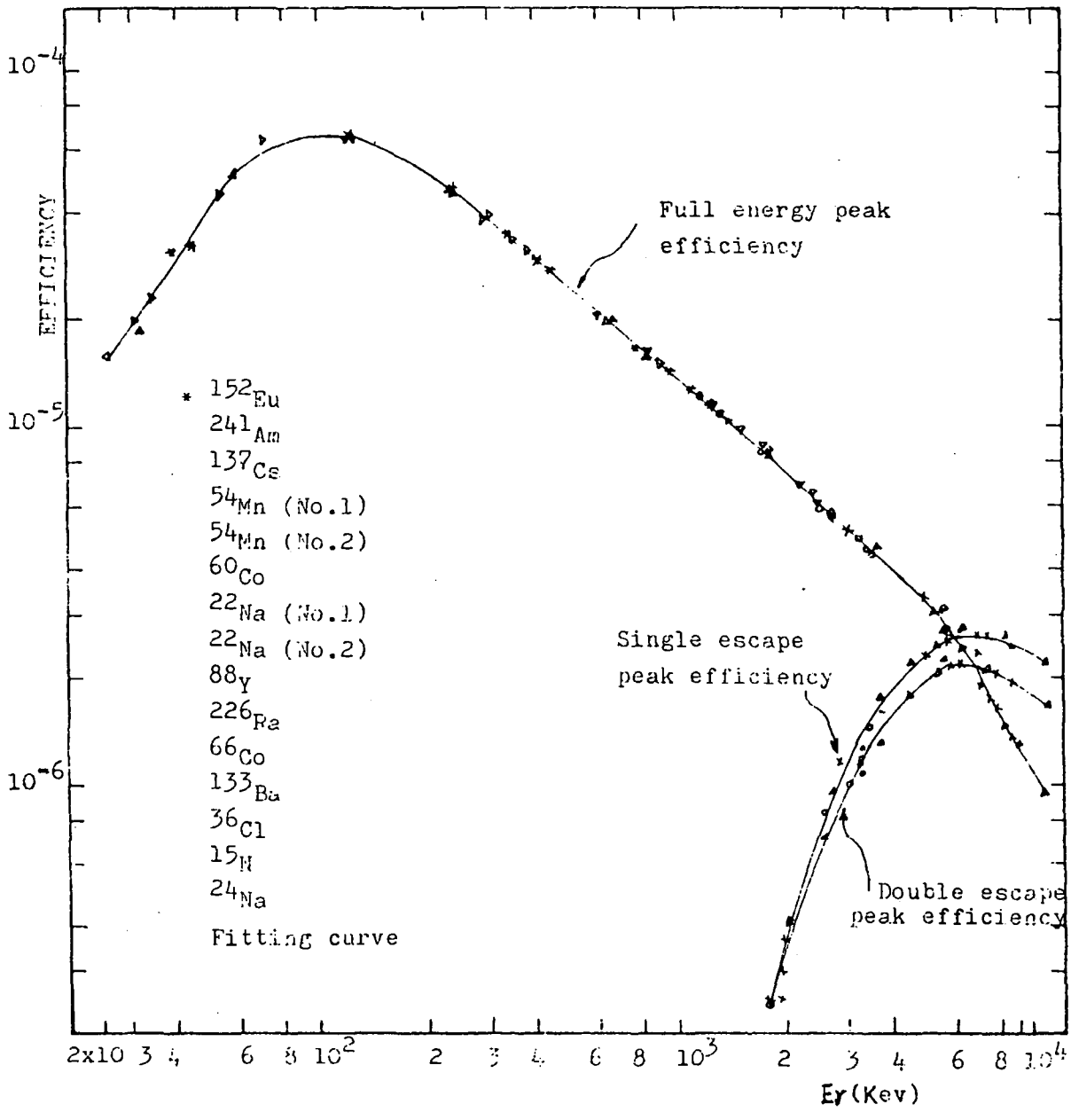

Fig.3 The efficiency curve for coaxial Ge(Li) detector with sensitivity volume 110.7cm^3

correct measurement results. 7 ways data acquisitions (γ ray energy spectra with fixed window width, variable window width and without window (ADC1, ADC3), α energy spectrum (ADC2.4), neutron energy spectrum of the ST-451 liquid scintillator (ADO2.2), time spectra of Ge(Li) and plastic scintillator detectors (ADC2.3 and ADC2.1)) were used, not only the monitoring of the measurement process was greatly enhanced, but also the results of different ways may be compared each other. In order to remove disturbances from the other high and low frequency signal sources, the width of the gate

pulses and gating time were carefully selected, and the coincidence between the gating pulses and linear pulses works quite well, the problem of measurement of low energy γ ray smaller than 500KeV was better solved, so that the γ ray yields with an energy larger than 80KeV can be correctly measured through correcting, and the γ ray yields with an energy larger than 180KeV can be measured without any loss (see Fig.7). The steps of the measuring as follows: in the first step the spectra with the sample were measured, in the second step the backgroud spectra of activation were measured, in the third step the background spectra without the samples were measured. The γ ray spectra for C, Al, V, Fe, Nb samples were shown in Fig.8-12. The time-of-flight spectra of γ-rays for $Fe(n,n'\gamma)$ and $C(n,n'\gamma)$ reaction were respectively shown in Fig.5-6.

Data Reduction

The discrete γ ray differential production cross-sections at θ angle with E_γ energy were calculated by the following formula

$$\frac{d\sigma}{d\Omega}(E_\gamma,\theta)=\frac{N_\gamma(E_\gamma,\theta)}{4\pi\phi_n N\varepsilon(E_\gamma)}f \qquad (1)$$

where $N(E_\gamma,\theta)$ is the counts in the full energy peak which was determined by means of Canberra S-80 multichannel analyzer and spectrum-F program after the background spectrum without the sample had been subtracted from the relevant γ ray spectrum with the sample, ϕ_n was obtained from the counts of α particles and can be calculated by the following formula:

$$\phi_n=\frac{\Omega_s N_\alpha A_\alpha}{\Omega_\alpha} \qquad (2)$$

in which Ω_s and Ω_α are the solid angle subtended by the sample and the α particle detector with respect to the neutron target respectively, N_α is the counts of α particles, A_α is anisotropy factor of neutron emittance from $T(D,n)^4He$ source, N is the sample thickness in the unit of atoms per cm^2 at the neutron incident direction, $\varepsilon(E_\gamma)$ is the absolute detection efficiency for full energy peaks of the Ge(Li) detector, f is the correction factor which includes the following several corrections.

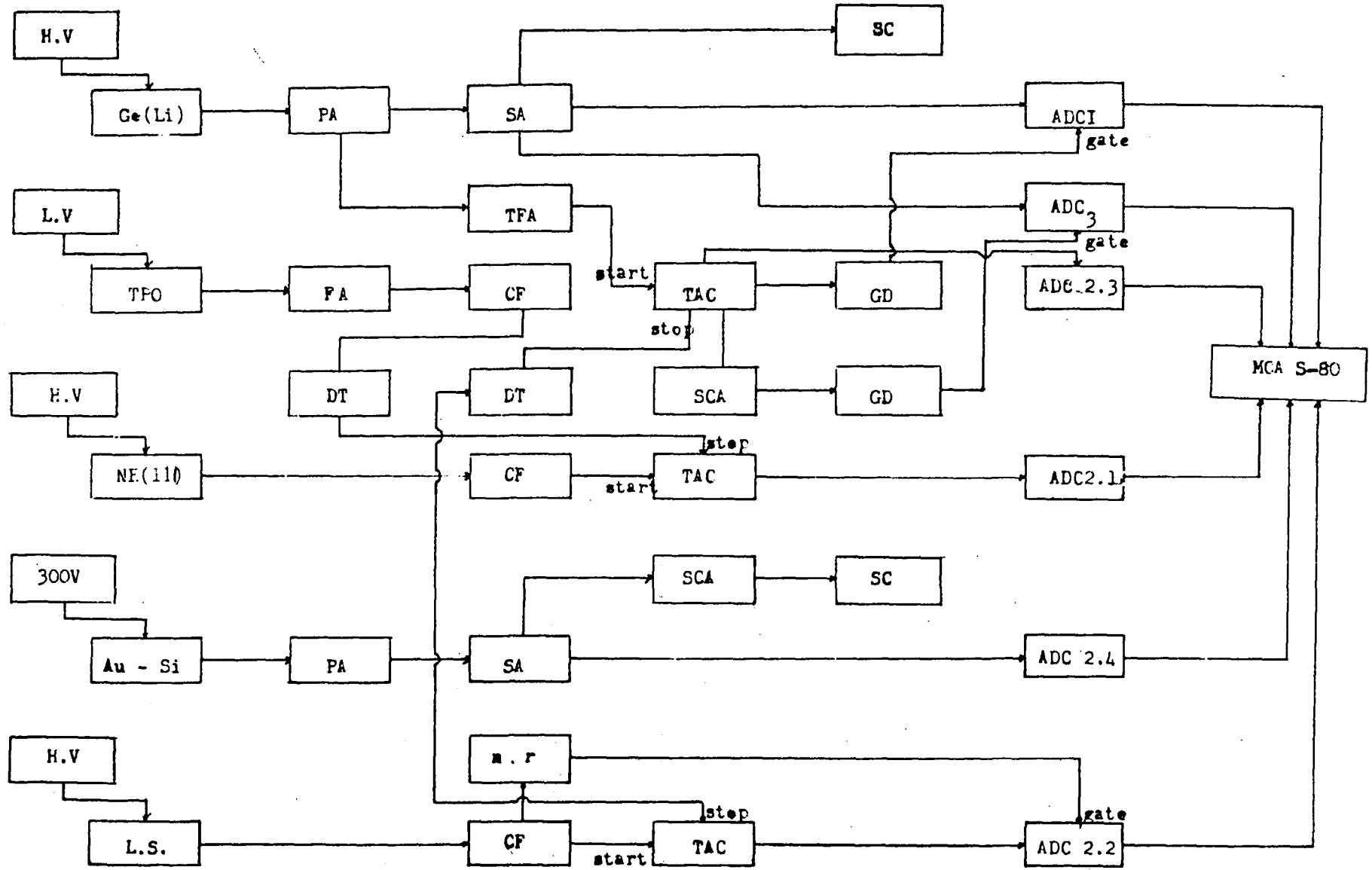
H.V
Ge(Li)
PA
SA
SC
ADCI
gate
L.V
TFA
ADC3
gate
TPO
FA
CF
start
TAC
GD
ADC 2.3
stop
MCA S-80
H.V
DT
DT
SCA
GD
stop
NE(110)
CF
start
TAC
ADC2.1
300V
SCA
SC
Au - Si
PA
SA
ADC 2.4
H.V
n . r
stop
gate
L.S.
CF
start
TAC
ADC 2.2

The abbreviations for Fig.4 are the following:

ADC = Analog-todigital converter
CF = Constant fraction timing
DT = nsec delay
FA = fast amplifier
GD = Gate and delay gernerator
MCA = Mulatichannel analyzer
N,r = Neutron-r discriminator
PA = Preamplifier
SA = Spectroscopy amplifier
SC = Scaler
SCA = Single channel analyzer
TAC = Time-toamplitude converter
TFA = Timing filtering amplifier
TPO = Time pickoff

Fig.4 The electronic block diagram for the (n,xr) reaction experiments

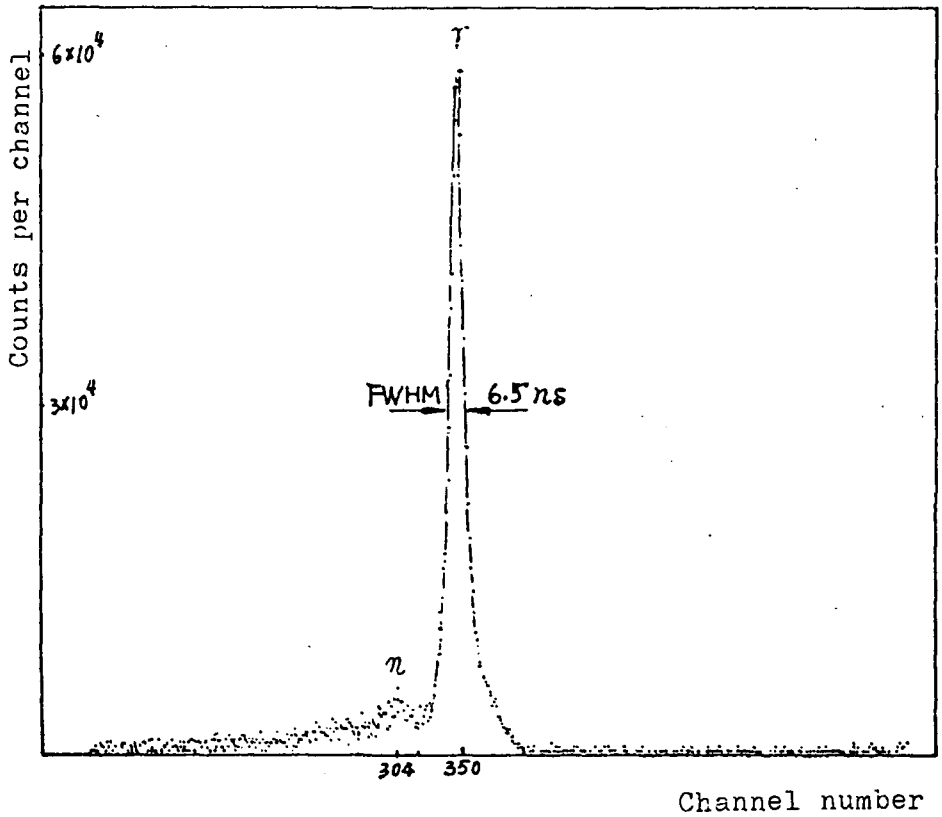

Fig.5 The time-of-flight spectrum of r-rays for Fe(n,n'r) reaction.

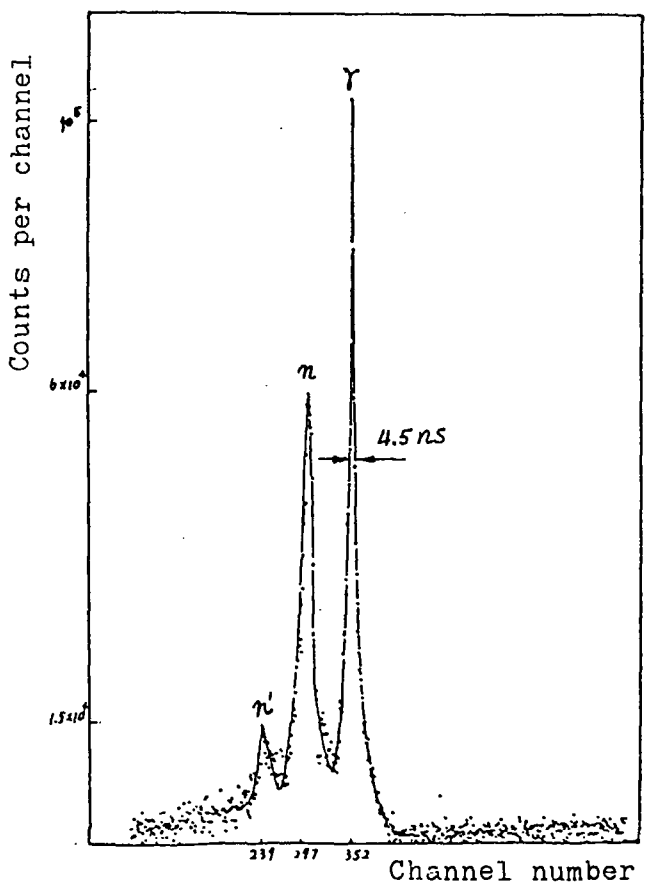

Fig.6 The time-of-flight spectrum of r-rays for C(n,n'r) reaction.

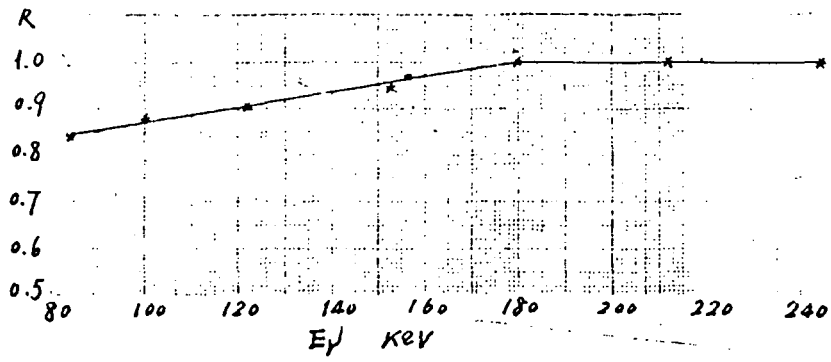

Fig.7 The relative count loss curve in the timing channel of the Ge(Li) detector.

(1) Neutron attenuation in the backing and cooling water of the neutron target, which was estimated to be 2.5%.

(2) Neutron attenuation in the sample, which was computed from the following formula

$$\int dRd\varphi f_R(R)/\int dRd\varphi fn(R,\varphi)-1 \tag{3}$$

in which

$$\int dRd\varphi = \int_{-\arcsin\frac{RC}{D}}^{\arcsin\frac{RC}{D}} \int_{D\cos\varphi-\sqrt{RC^2-D^2\sin^2\varphi}}^{D\cos\varphi+\sqrt{RC^2-D^2\sin^2\varphi}} dRd\varphi \tag{4}$$

$$f_R(R)=\frac{1}{R} \tag{5}$$

$$fn(R,\varphi)=\frac{\exp\left[-\mu n\left(R-D\cos\varphi+\sqrt{RC^2-D^2\sin^2\varphi}\right)\right]}{R} \tag{6}$$

where RC is the radius of the sample, D is the distance between the centre of the neutron target and the centre of the sample, R is the distance from the centre of the neutron target to the ds in the sample, φ is the angle between the connecting line from the centre of the neutron target to the centre of the sample and that from the centre of the neutron target to the ds in the sample (see Fig.13). The values of the neutron attenuation for the C, Al, V, Fe, Nb sample are respectively 16.3%, 13.5%, 20%, 21.8% and 28.7%.

(3) Neutron multiple scattering in the sample, was calculated using the semiempirical method proposed by C.A.Engelbrecht[1],[2]. But in the

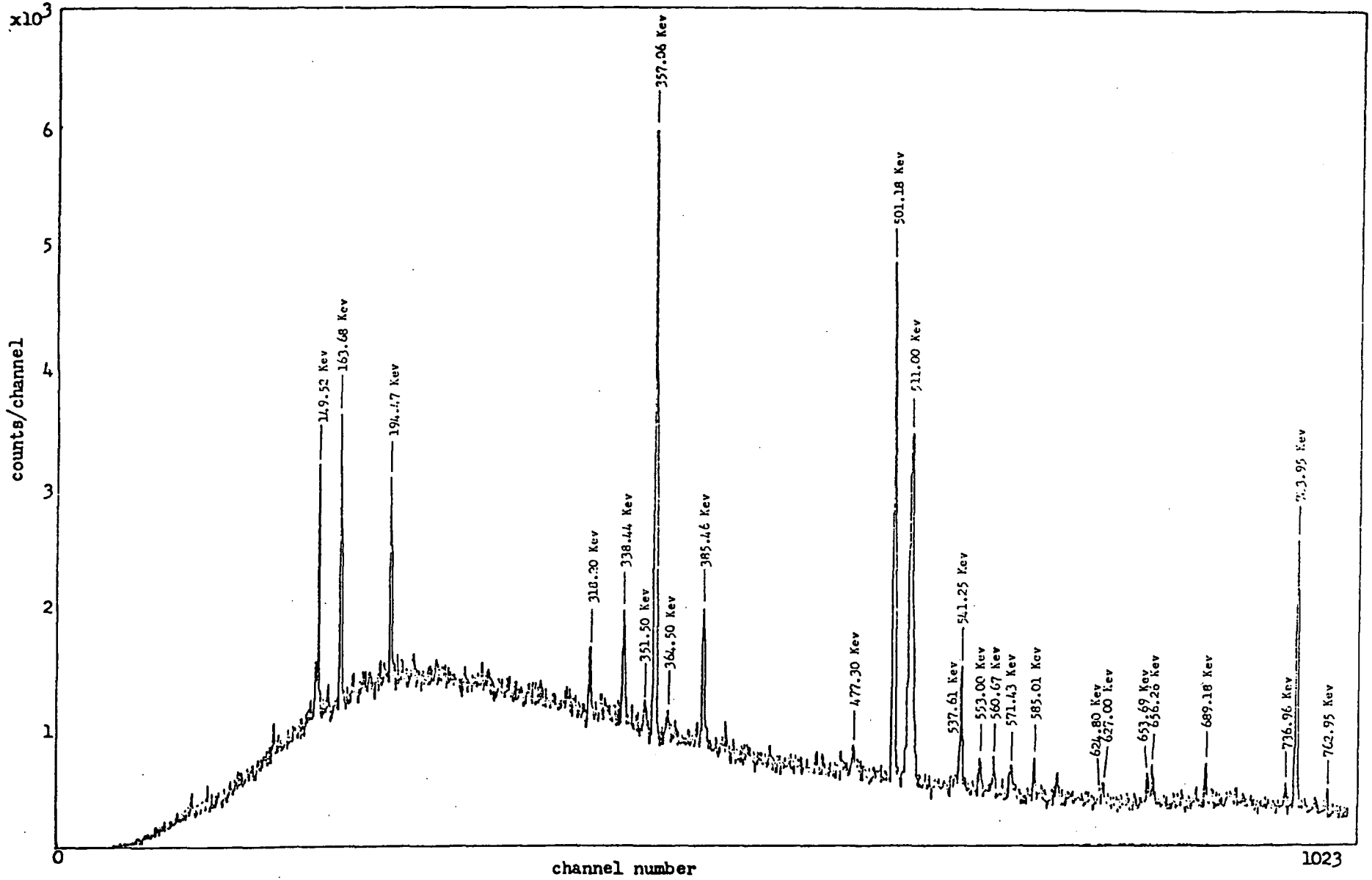

Fig. 8. Gamma radiation pulse height spectrum for $^{93}Nb(n,x\gamma)$ reaction at En=14.9 Mev and 90°

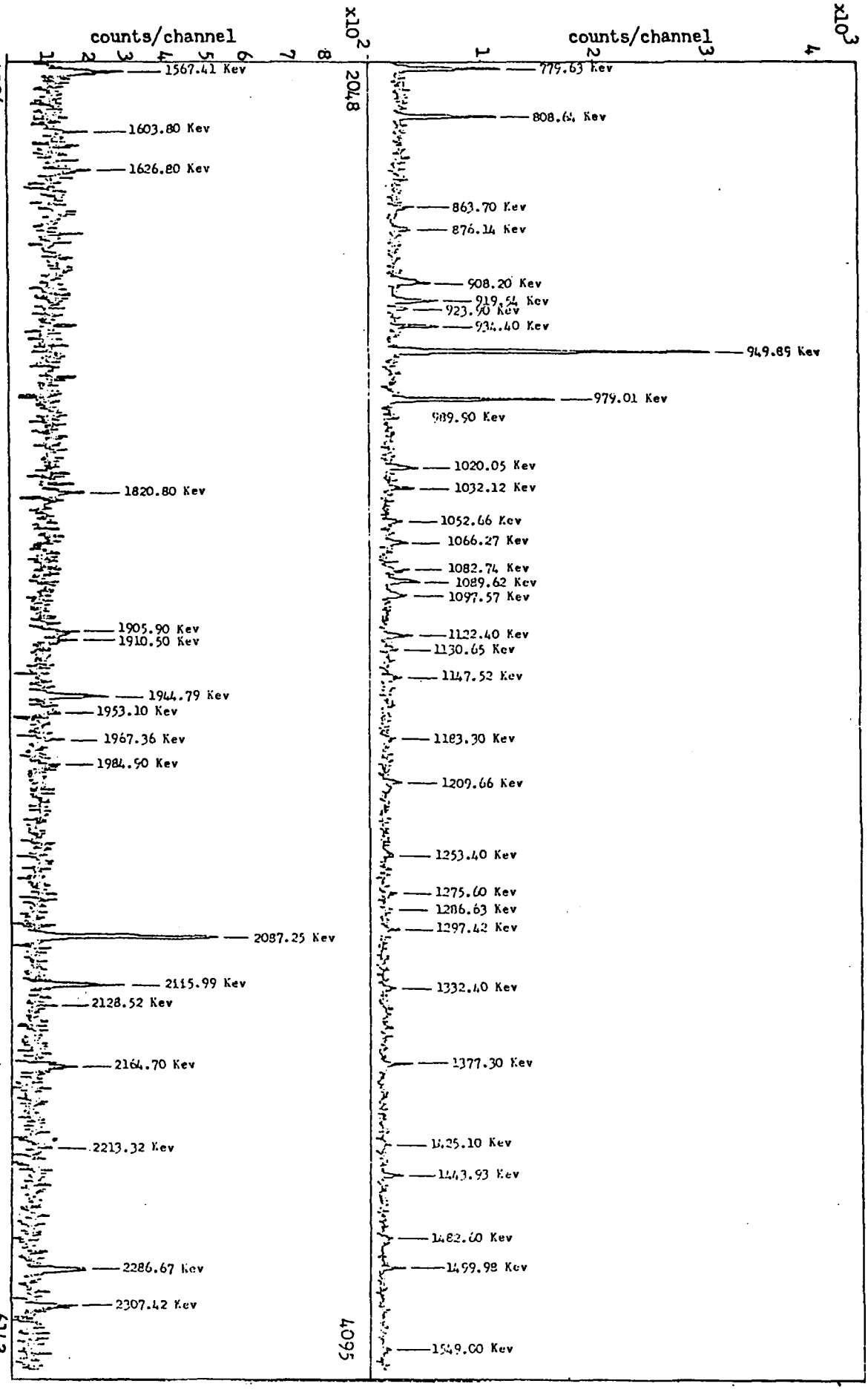
counts/channel
x10²
counts/channel
x10³
4096
2048
4095
6143
channel number
1567.41 Kev
1603.80 Kev
1626.80 Kev
1820.80 Kev
1905.90 Kev
1910.50 Kev
1944.79 Kev
1953.10 Kev
1967.36 Kev
1984.90 Kev
2087.25 Kev
2115.99 Kev
2128.52 Kev
2164.70 Kev
2213.32 Kev
2286.67 Kev
2307.42 Kev
779.63 Kev
808.64 Kev
863.70 Kev
876.14 Kev
908.20 Kev
919.54 Kev
923.90 Kev
934.40 Kev
949.89 Kev
979.01 Kev
989.90 Kev
1020.05 Kev
1032.12 Kev
1052.66 Kev
1066.27 Kev
1082.74 Kev
1089.62 Kev
1097.57 Kev
1122.40 Kev
1130.65 Kev
1147.52 Kev
1183.30 Kev
1209.66 Kev
1253.40 Kev
1275.60 Kev
1286.63 Kev
1297.42 Kev
1332.40 Kev
1377.30 Kev
1425.10 Kev
1443.93 Kev
1482.60 Kev
1499.98 Kev
1549.00 Kev

Fig. 8 (cont.)

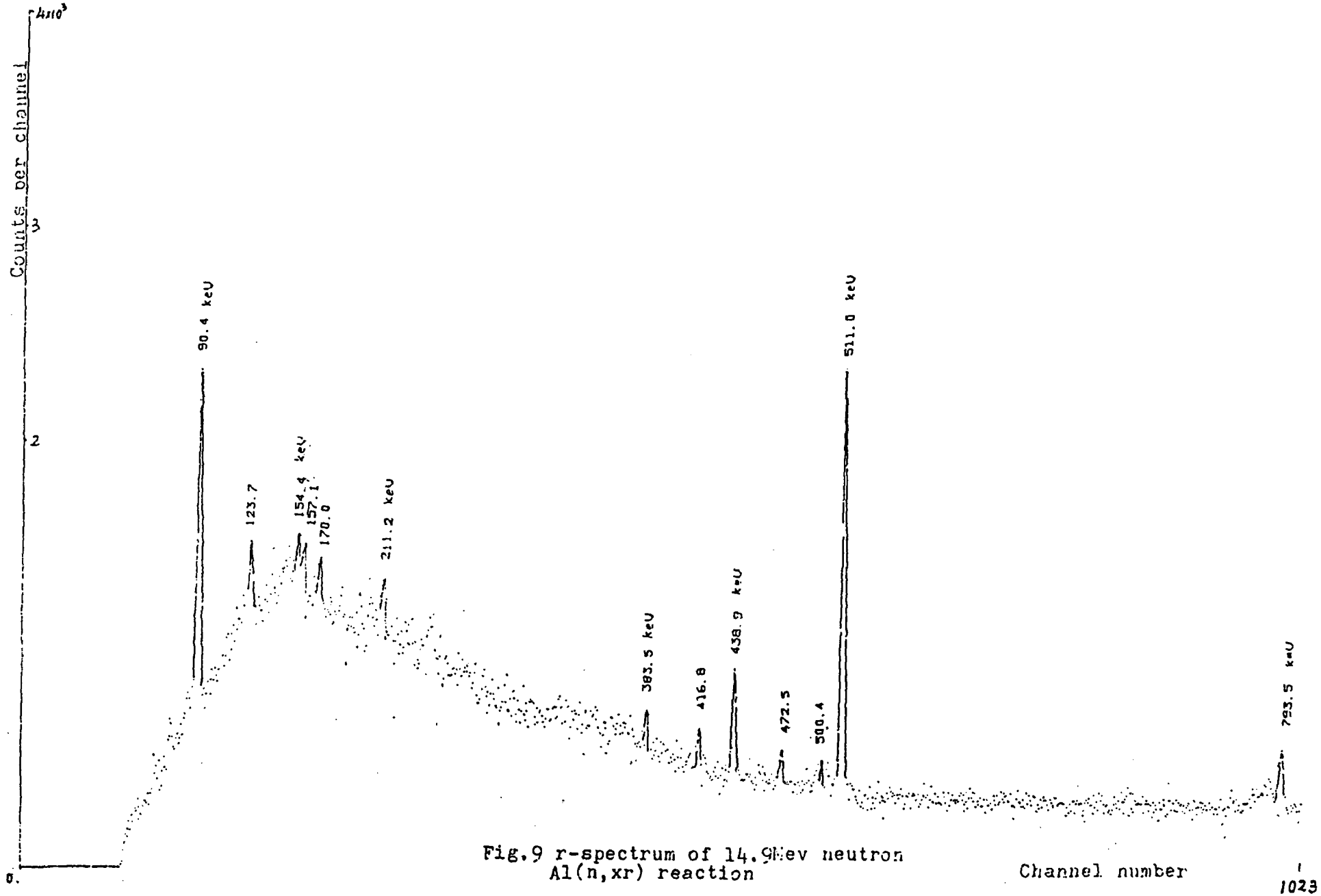

Fig.9 r-spectrum of 14.9Mev neutron
Al(n,xr) reaction

Counts per channel
2x10³
843.8 keV
862.7
868.8
873.4 keV
955.2 keV
961.6
984.2
1002.6
1014.0
keV
1129.3 keV
1172.1
1296.8 keV
1367.5
1506.1 keV
1024
2047
1698.1 keV
1719.8
1944.1 keV
2062.2
2210.6 keV
2298.6
2491.7
3004.0 keV
2048
4095
Channel number

Fig. 9 (cont.)

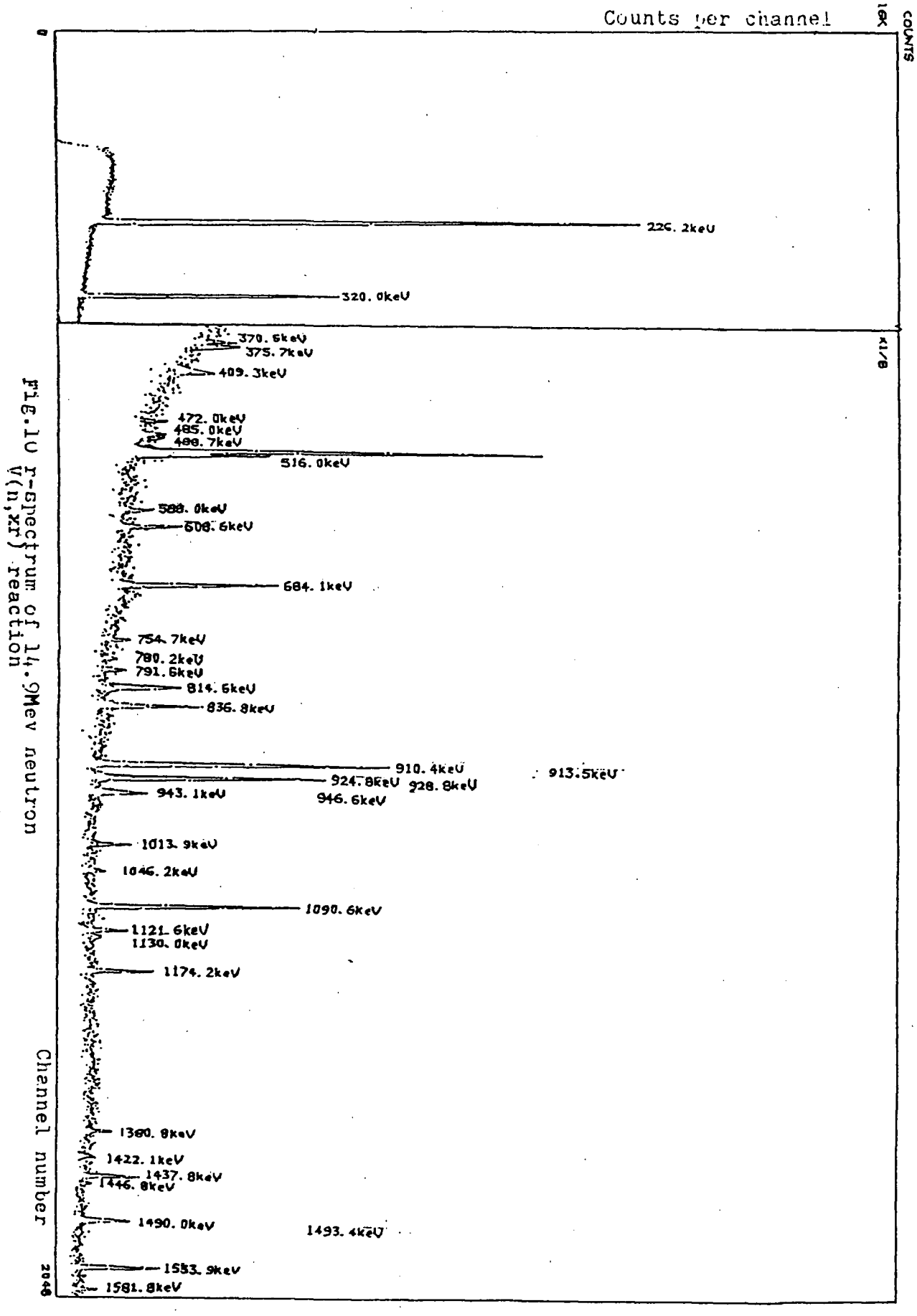

Fig.10 γ-spectrum of 14.9Mev neutron
W(n,xγ) reaction

COUNTS
4096
x1/2
Counts per channel
1609.4keV
1725.1keV
1748.5keV
1776.7keV
1785.3keV
1801.9keV
1813.2keV
2004.6keV
2024.8keV
2062.7keV
2110.2keV
2130.0keV
2292.3keV
2333.8keV
2351.8keV
2411.7keV
2049
Channel number
4096

Fig. 10 (cont.)

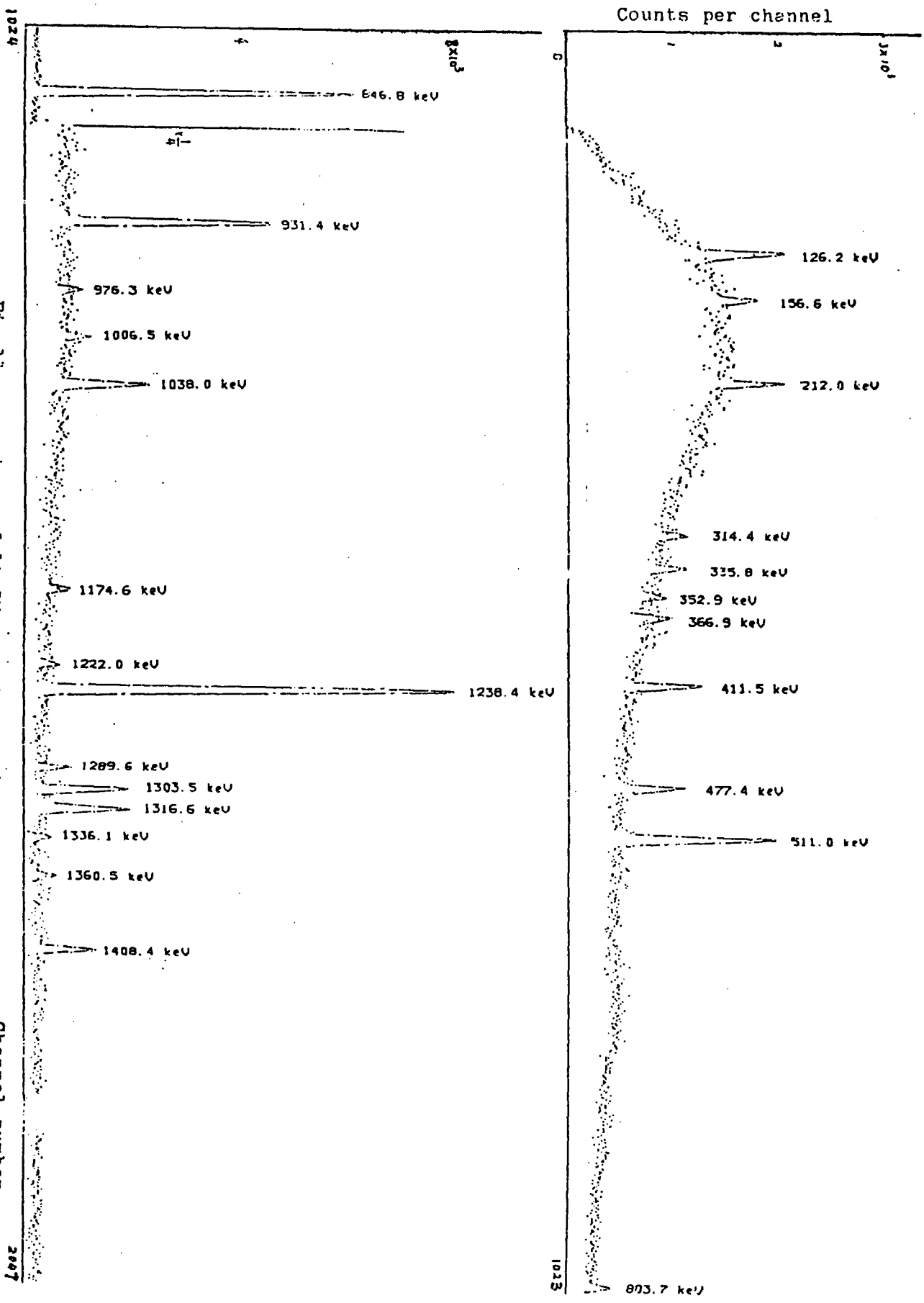

Fig.11 r-spectrum of 14.9Mev neutron Fe(n,xr) reaction.

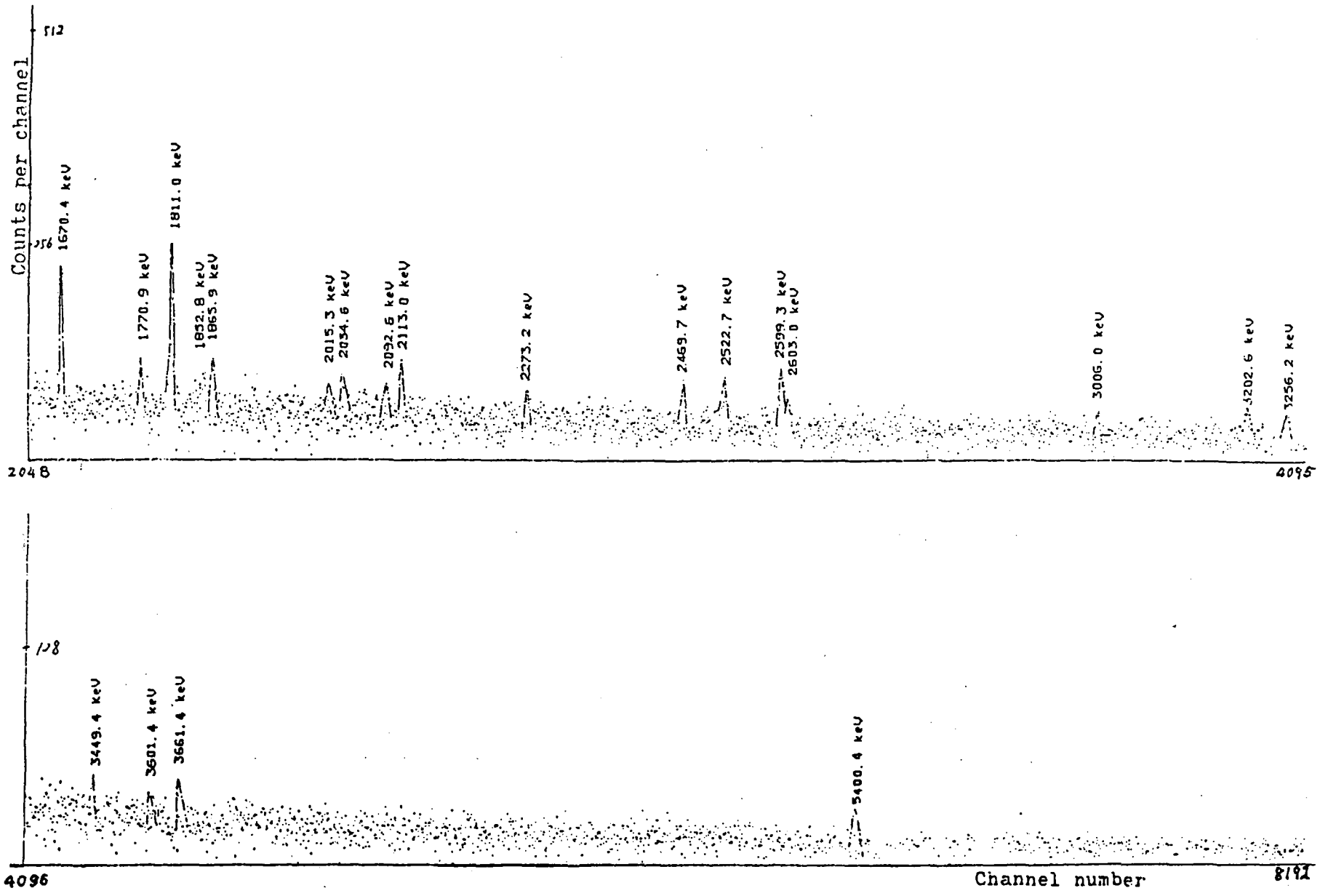
Counts per channel
512
256
128
1670.4 keV
1770.9 keV
1811.0 keV
1852.8 keV
1865.9 keV
2015.3 keV
2034.6 keV
2092.6 keV
2113.0 keV
2273.2 keV
2469.7 keV
2522.7 keV
2599.3 keV
2603.0 keV
3006.0 keV
3202.6 keV
3256.2 keV
3449.4 keV
3601.4 keV
3661.4 keV
5400.4 keV
2048
4095
4096
8192
Channel number

Fig. 11 (cont.)

Fig.12 r-spectrum of 14.9Mev neutron C(n,n'r) reaction

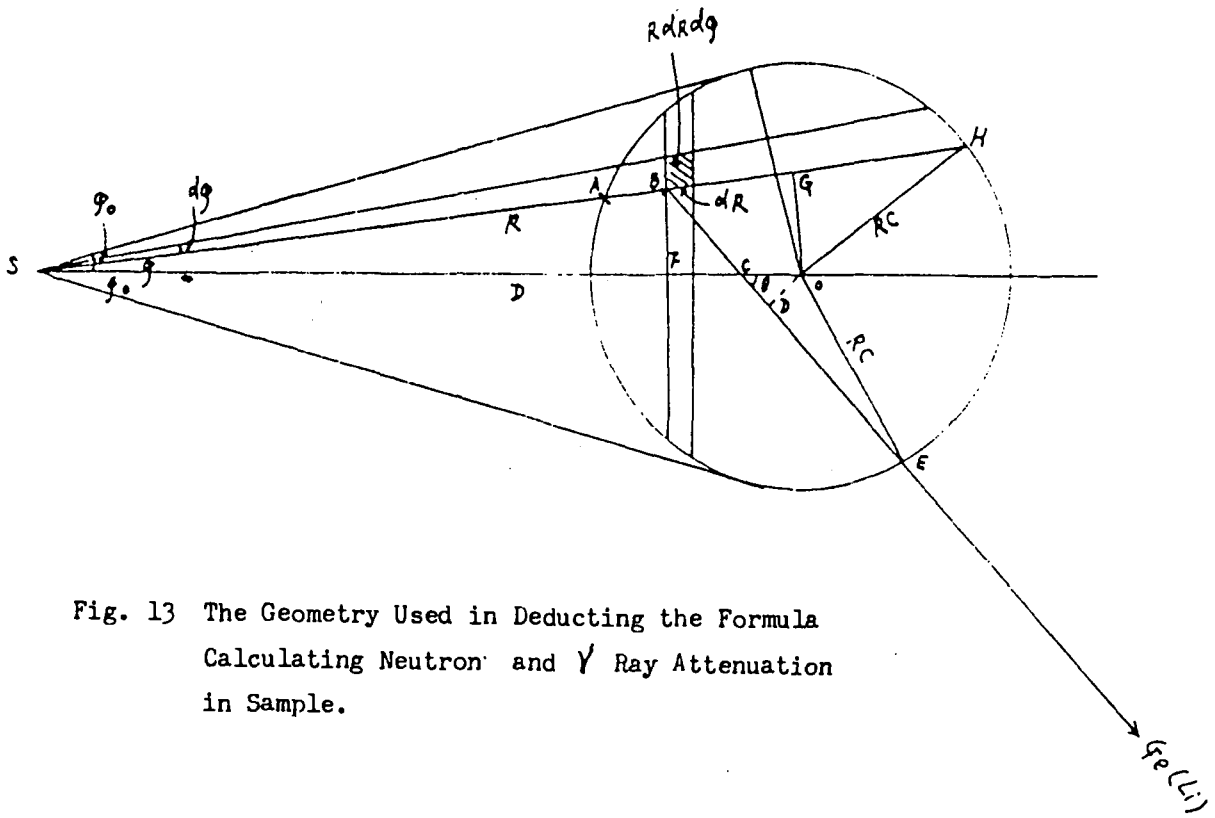

Fig. 13 The Geometry Used in Deducting the Formula Calculating Neutron and γ Ray Attenuation in Sample.

correction of multiple inelastic scattering the neutron inelastic scattering cross sections were replaced by γ ray production cross sections. The values of multiple elastic scattering corrections were 6.0% for C, 3.3% for Al, 5.1% for V, 5.7% for Fe, 8.1% for Nb and the values of inelastic scattering corrections were 1.8% for C, 3.3-4.5% for Al, 0.17-3.4% for V, 0.1-6.0% for Fe, 0.01-2.5% for Nb.

(4) γ ray attenuation in the sample, which was computed using the method proposed by Boring (1960). The formula is following

$$\int dR d\varphi f_R(R) / dR d\varphi f_\gamma(R,\varphi,\theta) - 1 \qquad (7)$$

where

$$f_\gamma(R,\varphi,\theta) = \exp\left\{-\mu_\gamma(E_\gamma)\left[\frac{R\sin\varphi}{\sin\theta} + (D - R\cos\varphi - R\sin\varphi\operatorname{ctg}\theta)\cos\theta + \sqrt{RC^2 - (D - R\cos\varphi - R\sin\varphi\operatorname{ctg}\theta)^2\sin^2\theta}\right]\right\} \qquad (8)$$

in which $\mu_\gamma(E_\gamma)$ is the macro absorption cross-section of the γ ray with an energy of E_γ in the sample and θ is the angle between the link from the centre of the neutron target to the centre of the sample and the derection from the sample to the centre of the Ge(Li) detector. The values of γ ray attenuation correction in the samples were 6.5% for C, 58-112% for Al, 33-655% for V, 127-315% for Fe, 46.8-1104% for Nb.

Table 1.

90^{o} differential production cross sections of the separate gamma-rays from interaction of 14.9Mev neutrons with C,Al,V,Fe,Nb samples

I. C

No.	Er(Kev)	probable reaction	suggested transition in the final nucleus (Kev)	isotopic cross section(mb/sr)
1	4439.0	$^{12}C(n,n'r)^{12}C$	4439.0--0	12.65±0.76

II. Al

No.	Er(Kev)	probable reaction	suggested transition in the final nucleus (Kev)	isotopic cross section(mb/sr)
1	90.4			2.14±0.20
2	123.7			0.78±0.17
3	154.4			0.29±0.08
4	157.1			0.25±0.08
5	170.0	$^{27}Al(n,n')^{27}Al$	1014.5--843.8	0.48±0.16
6	211.2			0.64±0.10
7	383.5			0.19±0.06
8	416.8	$^{27}Al(n,2n)^{26}Al$	416.9--0	0.36±0.08
9	438.9			1.04±0.10
10	472.5	$^{27}Al(n,\ )^{24}Na$	472.3--0	0.49±0.09
11	793.5	$^{27}Al(n,n')^{27}Al$	3004.2--2211.1	0.63±0.12
12	843.8	$^{27}Al(n,n')^{27}Al$	843.8--0	3.16±0.24
13	862.7	$^{27}Al(n,r)^{28}Al$	2485.0--1622.7	0.16±0.07
14	868.8	$^{27}Al(n,\ )^{24}Na$	1341.4--472.3	0.33±0.07
15	873.4			0.47±0.09
16	955.2			1.57±0.22
17	961.6			0.43±0.06
18	984.2	$^{27}Al(n,p)^{27}Mg$	984.6--0	2.54±0.23
19	1002.6	$^{27}Al(n,np)^{26}Mg$	3940.9--2938.4	0.34±0.09
20	1014.0	$^{27}Al(n,n')^{27}Al$	1014.5--0	7.41±0.55
21	1129.3	$^{27}Al(n,np)^{26}Mg$	2938.4--1808.7	2.12±0.18
22	1172.1			0.79±0.22
23	1296.8			0.99±0.33
24	1367.5	$^{27}Al(n,n')^{27}Al$	2211.1--843.8	0.65±0.13
25	1506.1	$^{27}Al(n,n')^{27}Al$	4510.3--3004.2	0.50±0.16
26	1698.1	$^{27}Al(n,p)^{27}Mg$	1698.3--0	2.37±0.23
27	1719.8	$^{27}Al(n,n')^{27}Al$	2734.9--1014.5	4.08±0.46
28	1808.1	$^{27}Al(n,np)^{26}Mg$	1808.7--0	13.98±0.99
29	1944.1			0.27±0.12

No.	Er(Kev)	probable reaction	suggested transition in the final nucleus (Kev)	isotopic cross section(mb/sr)
30	2062.2			0.33±0.16
31	2210.6	$^{27}Al(n,n')^{27}Al$	2211.1--0	9.51±0.76
32	2298.6	$^{27}Al(n,n')^{27}Al$	4510.3--2211.1	1.63±0.29
33	2491.7	$^{27}Al(n,p)^{27}Mg$	3476.1--984.6	0.22±0.08
34	3004.0	$^{27}Al(n,n')^{27}Al$	3004.2--0	2.64±0.81

III. V

No.	Er(Kev)	Probable reaction	Suggested transition in the final nucleus (Kev)	Isotopic cross section(mb/sr)
1	73.5			
2	85.5			0.49 ± 0.12
3	92.5			5.80 ± 0.55
4	94.5			5.15 ± 0.56
5	130.9			
6	134.7			
7	138.6			
8	226.2	$^{51}V(,,2n)$	226.2--0.0	35.03 ± 3.7
9	275.0			0.19 ± 0.15
10	320.0	$^{51}V(n,n')$	320.0--0.0	22.5 ± 2.4
11		$^{51}V(n,2n)$	320.2--000	
11	370.6			0.56 ± 0.14
12	375.7	$^{51}V(n,2n)$	1676.7--1300.7	0.45 ± 0.12
13	409.3			0.76 ± 0.13
14	472.0			0.13 ± 0.12
15	485.0	$^{51}V(n,2n)$		0.09 ± 0.09
16	488.7	$^{51}V(n,n')$	3873.7--3385.5	0.30 ± 0.17
17	516.0	$^{51}V(n,2n)$	836.4--320.2	2.82 ± 0.30
18	588.0			0.54 ± 0.12
19	608.6	$^{51}V(n,n')$	929.0--320.0	0.91 ± 0.14
20	684.1	$^{51}V(n,n')$	3377.8--2699.6	3.61 ± 0.43
		$^{51}V(n,2n)$	910.1--226.2	
21	754.1	$^{51}V(n,2n)$	2481.0--1725.0	0.51 ± 0.37
22	780.2			0.35 ± 0.19
23	791.6	$^{51}V(n,2n)$	1700.0--910.1	0.49 ± 0.14
24	814.6	$^{51}V(n,2n)$	1725.0--910.1	1.81 ± 0.25
25	836.8	$^{51}V(n,2n)$	836.4--0.0	2.91 ± 0.31
26	910.4	$^{51}V(n,2n)$	910.1--0.0	8.07 ± 0.90

No.	Er(Kev)	Probable reacrion	Suggested transition in the final nucleus (Kev)	Isotopic cross section(mb/sr)
27	913.5	$^{51}V(n,2n)$	1300.7--387.9	0.76 ± 0.22
28	924.8	$^{51}V(n,n')$	3873.7--2697.6	5.11 ± 0.98
29	928.8	$^{51}V(n,n')$	929.0--0.0	0.53 ± 0.06
30	934.1	$^{51}V(n,2n)$	1331.1--355.2	0.45 ± 0.13
31	946.6	$^{51}V(n,n')$	4821.0--3874.0	1.64 ± 0.22
		$^{51}V(n,2n)$	1300.7--355.2	
32	1013.9	$^{51}V(n,2n)$	1401.7--387.9	0.84 ± 0.22
33	1046.2	$^{51}V(n,2n)$	1401.7--355.2	0.89 ± 0.25
34	1090.6	$^{51}V(n,n')$	2698.0--1609.0	5.67 ± 0.60
35	1121.6			1.22 ± 0.23
36	1130.0	$^{51}V(n,2n)$	1518.0--387.9	0.41 ± 0.15
37	1174.2	$^{51}V(n,n')$	2874.0--1700.0	2.09 ± 0.22
38	1380.8	$^{51}V(n,2n)$	1700.7--320.0	0.76 ± 0.18
39	1422.1	$^{51}V(n,2n)$	1810.4--387.9	0.55 ± 0.33
40	1437.8			1.94 ± 0.22
41	1446.8	$^{51}V(n,n')$	4661.0--3215.0	0.20 ± 0.07
42	1490.0	$^{51}V(n,n')$	1810.0--320.0	0.26 ± 0.17
43	1493.4	$^{51}V(n,n')$	1813.0--320.0	2.36 ± 0.34
		$^{51}V(n,2n)$	1810.4--320.2	
44	1553.9	$^{51}V(n,2n)$	1553.9--0.0	2.86 ± 0.35
45	1581.8	$^{51}V(n,n')$		0.94 ± 0.22
46	1609.4	$^{51}V(n,n')$	1609.3--0.0	19.98 ± 2.10
47	1616.6			0.28 ± 0.11
48	1725.1	$^{51}V(n,2n)$	1725.0--0.0	0.72 ± 0.25
49	1748.5	$^{51}V(n,n')$	2677.3--929.0	0.39 ± 0.12
50	1776.7	$^{51}V(n,n')$	3385.5--1609.3	2.29 ± 0.37
51	1785.3			0.50 ± 0.19
52	1801.9	$^{51}V(n,n')$	3614.1--1813.0	0.46 ± 0.13
53	1813.2	$^{51}V(n,n')$	1813.0--0.0	6.47 ± 0.69
54	2004.6	$^{51}V(n,n')$	3614.1--1609.3	1.89 ± 0.41
55	2062.7	$^{51}V(N,2n)$	3553.0--1490.0	0.54 ± 0.21
56	2110.1			0.85 ± 0.13
57	3130.0			0.29 ± 0.21
58	2292.3			0.83 ± 0.24
59	2333.8	$^{51}V(n,n')$	3266.0--929.0	1.54 ± 0.20
60	2351.8	$^{51}V(n,n')$	3280.0--929.0	0.76 ± 0.21
61	2411.7	$^{51}V(n,n')$		0.69 ± 0.13

IV. Fe

No.	Er(Kev)	probable reaction	suggested transition in the final nucleus (Kev)	isotopic cross section(mb/sr)
1	126.2			5.41±1.02
2	156.6			1.59±0.49
3	212.0			2.58±0.52
4	314.4			0.93±0.38
5	335.8			1.54±0.47
6	352.9	^{57}Fe(n,n')	366.7--14.4	50.38±20.49
7	366.9	^{56}Fe(n,n')	3755.5--3388.8	1.06±0.40
8	411.5	^{56}Fe(n,2n)	411.3--0	4.47±0.59
9	477.4	^{56}Fe(n,2n)	1408.5--931.4	5.40±0.71
10	803.7	^{56}Fe(n,2n)	2211.9--1408.5	1.76±0.46
		^{56}Fe(n,n')	4660.0--3856.5	
11	846.8	^{56}Fe(n,n')	846.8--0	65.42±4.57
12	931.4	^{56}Fe(n,2n)	931.4--0	11.72±0.49
13	976.3	^{56}Fe(n,n')	4100.3--3122.9	0.44±0.28
14	1006.5	^{56}Fe(n,n')	4395.0--3388.8	1.79±0.57
15	1038.0	^{56}Fe(n,n')	3122.9--2085.1	5.86±0.63
16	1174.6	^{56}Fe(n,n')	3832.0--2657.5	0.70±0.36
17	1238.4	^{56}Fe(n,n')	2085.1--846.8	29.66±2.10
18	1289.6			1.58±0.36
19	1303.5	^{56}Fe(n,n')	3388.8--2085.1	5.74±0.57
20	1316.5	^{56}Fe(n,2n)	1316.8--0	6.16±0.65
21	1336.1	^{56}Fe(n,n')	4458.4--3122.9	0.82±0.27
22	1360.5	^{56}Fe(n,n')	3445.4--2085.1	0.72±0.24
23	1408.4	^{56}Fe(n,2n)	1408.5--0	4.37±0.48
24	1670.4	^{56}Fe(n,n')	3755.5--2085.1	3.95±0.49
25	1770.9	^{56}Fe(n,n')	3856.5--2085.1	1.17±0.46
26	1811.0	^{56}Fe(n,n')	2657.5--846.8	5.38±0.64
27	1852.8			0.56±0.37
28	1865.0			1.21±0.34
29	2015.3	^{56}Fe(n,n')	4100.3--2085.1	0.61±0.33
30	2034.6	^{56}Fe(n,n')	4120.0--2085.1	1.04±0.33
31	2092.6			0.53±0.37
32	2113.0	^{56}Fe(n,n')	2959.9--846.8	1.89±0.46
33	2273.2	^{56}Fe(n,n')	3120.0--846.8	0.64±0.45
34	2469.7			1.71±0.45
35	2522.7	^{56}Fe(n,n')	3369.7--846.8	1.65±0.51
36	2599.3	^{56}Fe(n,n')	3445.3--846.8	3.03±0.57
37	2603.0	^{56}Fe(n,n')	3449.3--846.8	1.33±0.39
38	3202.6	^{56}Fe(n,n')	4049.0--846.8	0.81±0.36
39	3252.2			1.42±0.54
40	3449.4	^{56}Fe(n,n')	3449.3--0	0.75±0.39
41	3661.4	^{56}Fe(n,2n)	3661.0--0	0.84±0.30

V. Nb

No.	Eγ(Kev)	Probable Reaction	Final Nucleus Transition(Kev)	Isotopic cross Section(mb/sr)
1	149.52	(n,2n)	285.0--135.1	22.45 ± 2.10
2	163.68	(n,2n)	389.1--225.0	15.87 ± 1.52
3	194.47	(n,2n)	479.6--285.0	8.72 ± 0.84
4	318.20	(n,n')	1082.68--743.91	
			2003.38--1686.07	0.919 ± 0.150
			1297.32--979.06	
		(n,2n)	1642.0--1324.0	
5	338.44	(n,n')	1082.68--743.91	
			2003.38--1665.76	3.17 ± 0.29
6	351.50			1.19 ± 0.45
7	357.06	(n,2n)	357.06--0.0	19.76 ± 1.09
8	364.50	(n,2n)	1679.56--1315.08	0.362 ± 0.330
9	385.46	(n,n')	1334.80--949.50	5.69 ± 0.40
10	477.3	(n,n')	1968.25--1949.15	1.12 ± 0.42
11	501.18	(n,2n)	501.0--0.0	21.78 ± 1.23
12	537.61	(n,n')	2003.2--1665.76	0.594 ± 0.095
13	541.25	(n,n')	1491.15--949.50	4.13 ± 0.32
14	553.00	(n,n')	1297.32--743.91	
			1497.80--1394.61	1.46 ± 0.45
		(n,2n)	1642.0--1089.0	
15	560.67	(n,n')	1369.41--810.15	1.53 ± 0.37
16	571.43	(n,n')	1315.08--743.91	1.10 ± 0.18
17	585.01	(n,n')	1394.61--810.05	1.12 ± 0.24
18	624.80			1.00 ± 0.23
19	627.00			0.617 ± 0.235
20	653.69	(n,n')	1602.80--949.50	1.14 ± 0.15
21	656.26	(n,n')	686.44-- 30.40	1.57 ± 0.20
22	689.18	(n,n')	2171.98--1483.37	2.23 ± 0.46
23	736.96	(n,n')	1686.07--949.50	0.757 ± 0.334
24	743.95	(n,n')	743.95--0.0	13.17 ± 0.80
25	762.95	(n,2n)	2998.0--2235.0	1.23 ± 0.18
			1738.0--975.0	
26	779.63	(n,n')	1728.59--949.50	4.93 ± 0.43
			810.05--30.40	
27	808.64	(n,n')	808.64--0.0	4.70 ± 0.32
		(n,2n)	1310.0--510.0	

No.	E_γ(Kev)	Probable Reaction	Final Nucleus Transition(Kev)	Isotopic Cross Section(mb/sr)
28	863.7	(n,2n)	1089.0--225.3	0.636 ±0.267
29	876.14	(n,n')	2367.31--1491.15	1.04 ± 0.27
30	908.20	(n,2n)	1410.2--501.0	2.43 ± 0.33
31	919.54	(n,n')	949.50--30.40	2.89 ± 0.40
			1728.59--808.69	
32	923.90			1.12 ± 0.24
33	934.40	(n,2n)	1414.0--479.6	2.98 ± 0.35
34	949.89	(n,n')	949.89--0.0	21.25 ± 1.11
			2203.2--1253.79	
35	979.01	(n,n')	979.01--0.0	9.27 ± 0.57
36	989.90	(n,n')	1968.2500979.06	1.41 ± 0.29
37	1020.05	(n,n')	1968.25--949.50	2.33 ± 0.23
38	1032.12	(n,n')	2367.31--1334.80	
			2329.90--1297.52	1.84 ± 0.19
		(n,2n)	1422.0--389.1	
39	1052.66	(n,n')	2003.38--949.50	1.16 ± 0.36
40	1066.27			1.51 ± 0.32
41	1082.74	(n,n')	1082.74--0.0	1.35 ± 0.19
42	1089.62	(n,n')	2171.98--1082.68	1.81 ± 0.24
43	1097.57			1.27 ± 0.19
44	1122.4			2.46 ± 0.30
45	1130.65	(n,2n)	1632.0--501.0	1.92 ± 0.28
46	1147.52	(n,n')	2482.89--1334.80	1.57 ± 0.24
47	1183.30			0.881 ± 0.390
48	1209.66	(n,n')	2019.01--808.69	1.36 ± 0.37
49	1253.40	(n,n')	1253.40--0.0	0.713 ± 0.190
50	1275.60	(n,2n)	1411.0--135.1	1.86 ± 0.24
51	1286.63	(n,n')	2584.04--1297.32	1.23 ± 0.18
52	1297.42	(n,n')	1297.42-- 0.0	1.94 ± 0.21
53	1332.40			1.11 ± 0.28
54	1377.30			2.50 ± 0.24
55	1425.1			1.03 ± 0.32
56	1443.93	(n,2n)	1945.0--501.0	1.59 ± 0.32
57	1482.60	(n,n')	1482.60--0.0	1.03 ± 0.20
58	1499.98	(n,n')	1499.98--0.0	2.03 ± 0.22
59	1549.00			1.01 ± 0.23
60	1567.41			2.10 ± 0.23
61	1603.80			1.20 ± 0.50

No.	Eγ(Kev)	Probable Reaction	Final Nucleus Transition(Kev)	Isotopic Cross Section(mb/sr)
62	1626.80			0.980 ± 0.280
63	1820.80			1.28 ± 0.24
64	1905.90			1.70 ± 0.46
65	1910.50			1.23 ± 0.41
66	1944.79	(n,2n)	1944.79--0.0	1.70 ± 0.25
67	1953.10			0.952 ± 0.290
68	1967.36	(n,n')	1967.36--0.0	0.807 ± 0.210
69	1984.90			1.23 ± 0.41
70	2087.25	(n,2n)	2087.25--0.0	7.43 ± 0.42
71	2115.99			3.08 ± 0.35
72	2128.52			0.803 ± 0.130
73	2164.70	(n,2n)	3797.0--1632.0	1.16 ± 0.26
74	2213.32			0.981 ± 0.220
75	2286.67	(n,2n)	2286.67--0.0	3.10 ± 0.31
76	2307.42			1.88 ± 0.21
77	2407.35			1.02 ± 0.21
78	2432.28			0.875 ± 0.160
79	2507.50			0.916 ± 0.230

(5) Contribution of γ ray from activities produced by (n,p) and (n,2n) reactions. it was calculated by fullowing formula

$$N_A(E\gamma) = \frac{T_W}{T} \cdot \frac{\lambda C(E\gamma)\{(t_2 - t_1) + \frac{1}{\lambda}[e^{-\lambda(t_2 - t_0)} - e^{-\lambda(t_1 - t_0)}]\}}{[e^{-\lambda(t_4 - t_3)} - e^{-\lambda(t_5 - t_3)}][1 - e^{-\lambda(t_3 - t_0)}]} \qquad (9)$$

in which Tw is width of γ ray time window at the time of flight spectrum, T is a period of the neutron pulses, λ is the decay constant of the activated nuclide, C(Eγ) is γ ray peak counts at the activation background spectrum with an energy of Eγ, to is the start time of the neutron beams, t_1, t_2 are the start time and the stop time of measuring γ ray spectrum with the sample in beam respectively, t_3 is the time of stop beam, t_4, t_5 are the start time and the stop time of measuring activation background spectrum. For Instance the values of the activation background contribution were about 2% and 10% for 847KeV γ ray of Fe and for 934.4KeV γ ray of Nb which were produced by (n,p) and (n,2n) reactions respectively.

(6) The correction induced by size of the neutron target was 1.2%.

(7) γ ray count loss induced by the threshold of the timing channel of Ge(Li) detector and the gating time as well as width of gating pulses (see Fig.7). This correction was from o for E_γ = 180KeV to 16% for E_γ=80KeV.

(8) The effect of the dead time of measurement system was ignored because the count rates of γ rays and α particles were only about 100 counts per second.

The neutron cross sections to be used in the calculations of items(1), (2) and (3) were taken from ENDF B-IV, and the γ ray attenuation coefficients for item (4) were taken from Decay Scheme[3].

The errors of the obtained cross sections were estimated taking account of the uncertainties in

1. determining the counts $N_\gamma(E_\gamma)$ in the full energy peak, which depends on the individual γ ray peak(1%-100%).

2. determining the neutron flux ϕ_n of the incident upon the sample(4%).

3. absolute detection efficiency for full energy peaks $\varepsilon(E_\gamma)$ (1.5%-3.0%).

4. the correction factor f (1.0%-3.0%).

The discrete γ ray production cross section (including the total corrections metioned above) were computed by CG.FOR code, which was a improved edition from CORGAM.FOR code used in Accelerator Laboratory of Kentucky University.

In order to test the experimental facility, the experimental methods and the data processing methods three sample of Fe with different size were measured and computed, the results were agree with each other in the error range.

The discrete γ ray production cross sections for interactions of 14.9MeV neutrons with C, Al, V, Fe, Nb at 90° are summarized in Table 1. In the table probable reaction types and transitions were taken from level scheme in refs.(4).

Discussions

Although the discrete γ ray production cross sections for interactions of 14MeV neutrons with C, Al, Fe at 90° have had a lot of data[5]-[24] the discrepancy among those data is very large and the accuracy is also very poor, because the large part of these data were measured by means of NaI(Tl) detectors, and only the little part were measured by the smaller Ge(Li) detector with lower efficiency and energy resolution, so to determine the area of the full energy peaks was difficult. The data for the discrete γ ray production cross sections for interactions with V, Nb haven't been reported yet so far. The present data measured by means of the Ge(Li) with high efficiency and high resolution are a matter of interest for elimenating the discrepancy of previous data, filling in the data in some nuclides at 14MeV neutron energy and improving the level schemes of relative nuclides.

For C, only 4.439MeV γ ray peak was measured. The present result is slightly larger than the recent data[5]-[8] and near to the earlier measurement results[9],[11]-[13]. In Fig.12 4.439MeV peak is full energy peak of 4.439MeV γ ray which was emitted when first exitation state of ^{12}C transits to ground state of ^{12}C, 3.928MeV and 3.417MeV are its single escape peak and double escape peak respectively. Three peaks were broadened by Dopplor effect. Morethere, the phenomena that every peak breaks into two peaks was again discovered. its reasonable explanation havn't been seen so far. The research for this phenomena will be continued . The present data was given by considering the two peaks as one peak.

For Al 34 lines were obtained, in which 21 lines were found first in this type experiment. The present data agree with the those of ref.(5).

For Fe, 41 lines were obtained in which the those with an lower than 300KeV were first given, The present data agree with ref.(6), (9), (19), (20).

The discrete γ ray spectra for interactions of 14.9MeV neutrons with V, Nb were first measured, 61 lines for V and 79 lines for Nb were respectively obtained.

The angular distributions of the discrete γ ray spectra for interaction of 14.9MeV neutrons with C, Al, V, Fe, Co, Nb are being measured. The effects of some new lines discovered in present work are being studied.

Reference

(1) C.A.Engelbrecht Nucl. Inst. and Methods 80, 187 (1970)

(2) C.A.Engelbrecht Nucl. Inst. and Methods 93, 103 (1971)

(3) Liu Ying-Zang et al., Decay Scheme (1980)

(4) D.M.Lederer et al., Table of Isotopes (1978)

(5) Shi Zongren et al., CNP. 1, 45 (1979)

(6) D.W.Drake et al., Nucl, Sci. Eng 65, 49 (1978)

(7) G.L.Morgan et al., ORNL-TM 3702 (1972)

(8) D.Spaagaren et al., Nucl. Phys. A 161, 354 (1971)

(9) F.C.Engesser et al., J.Nucl. Energy. 21, 487 (1967)

(10) G.Clayeaaux et al., CEA-R-3807 (1969)

(11) D.T.Stewart et al., Nucl. Phys. 60, 349 (1964)

(12) J.Benveniste et al., Nucl. Phys., 19 448 (1960)

(13) J.D.Anderson et al., Phys. Rev., 111, 572 (1958)

(14) J.Lachkar et al., "An Evaluation of the neutron induced scattering, Reaction, and photo production cross section of carbon."

(15) A.P.Arya et al., Bull. Am. Phys. SOC. 12, 124 (1967)

(16) E.N.Cyxahob N P., ephax uzuka, 11, 33 (1970)

(17) J.T.Prudhomme et al., AFSWC-TR-60-30 (1960)

(18) M.D.Goldberg et al., BNL-400, 2nd, ed., (1962)

(19) J.Lachkar et al., Nucl. Sci. Eng. 55, 168(1974)

(20) U.Abbondanno et al., J.Nucl. Energy, 27, 227 (1973)

(21) G.Grenier Proc. Conf. on Neutron Phys., Kief 1972 Vol.3, 217 (1973)

(22) P.S.Buchanan et al., ORO-2791-32 (1971)

(23) P.W.Martin et al., Can.J.Phys., 46, 1657 (1968)

(24) P.W.Martin et al., J.Nucl. Energy 19, 447 (1965)

(25) G.E.Thomas et al., Nucl, Inst. and Methods 56, 325 (1967)